Graphene oxide derivatives as hole- and electron-extraction layers for high-performance polymer solar cells

Jun Liu,*[a] Michael Durstock[b] and Liming Dai*[c]

Owing to their solution processability, unique two-dimensional structure, and functionalization-induced tunable electronic structures, graphene oxide (GO) and its derivatives have been used as a new class of efficient hole- and electron-extraction materials in polymer solar cells (PSCs). Highly efficient and stable PSCs have been fabricated with GO and its derivatives as hole- and/or electron-extraction layers. In this review, we summarize recent progress in this emerging research field. We also present some rational concepts for the design and development of the GO-based hole- or electron-extraction layers for high-performance PSCs, along with challenges and perspectives.

Broader context

Owing to their solution processability, unique two-dimensional structure, and functionalization-induced tunable electronic structures, graphene oxide (GO) and its derivatives have been used as a new class of efficient hole- and electron-extraction materials in polymer solar cells (PSCs). Highly efficient and stable PSCs have been fabricated with GO and its derivatives as hole- and/or electron-extraction layers. In this review, we summarize recent progress in this emerging research field. We also present some rational concepts for the design and development of the GO-based hole- or electron-extraction layers for high-performance PSCs, along with challenges and perspectives.

1. Introduction

During the past decade or so, polymer solar cells (PSCs) have attracted a great deal of interest because of many competitive advantages, including their versatility for large-scale fabrication through the roll-to-roll process, flexibility, lightweight, and low cost.[1–9] Continued development of novel polymeric/organic materials, optimization of device structures, and improvement of fabrication techniques have steadily increased the power conversion efficiency (PCE) of PSCs up to >9% for single junction cells[10] and >10% for tandem cells.[11] In order for PSCs to be competitive with conventional photovoltaic technologies based on silicon or other inorganic materials, however, the efficiency and lifetime of PSCs still need to be significantly improved.

The photovoltaic effect involves generation of electrons and holes in a semiconductor device under illumination, and subsequent charge collection at opposite electrodes. Photon absorption of organic optoelectronic materials often creates bound electron–hole pairs (*i.e.* excitons). Charge collection, therefore, requires dissociation of the excitons, which occurs only at the heterojunction interface between semiconducting materials of different ionization potentials or electron affinities. Like many other polymeric thin film devices,[12] the interfaces in PSCs play critical roles in regulating the charge separation and charge collection, and hence the overall device performance.[13,14] For high-performance PSCs, the work functions of the cathode and the anode need to match the LUMO level of the acceptor and the HOMO level of the donor, respectively, to minimize energy barriers for electron- and hole-extraction. The energy barriers between the active layer and the electrodes can also be effectively reduced by electron-/hole-extraction layers at the cathode/anode. Therefore, a hole-extraction layer (HEL) between the anode and the active layer, as well as an electron-extraction layer (EEL) between the cathode and the active layer, are essential for achieving maximum PSC device efficiency and lifetime.[15–17] The functions of hole- and electron-extraction layers include: (i) to minimize the energy barrier for charge extraction; (ii) to selectively extract one sort of charge carrier and block the opposite charge carrier; (iii) to improve the interface stability between the electrode and the active layer; (iv) to modify the surface properties and alter the active layer morphology; and (iv) to act as an optical spacer.[15–17]

Several classes of materials, including organic conductive polymers (*e.g.* poly(3,4-ethylenedioxythiophene) doped with

[a]*State Key Laboratory of Polymer Physics and Chemistry, Changchun Institute of Applied Chemistry, Chinese Academy of Sciences, 5625 Renmin Street, Changchun 130022, P. R. China. E-mail: liujun@ciac.ac.cn*

[b]*Materials and Manufacturing Directorate, Air Force Research Laboratory, RXBP, Wright-Patterson Air Force Base, OH 45433, USA*

[c]*Center of Advanced Science and Engineering for Carbon (Case4Carbon), Department of Macromolecular Science and Engineering, Case Western Reserve University, 10900 Euclid Avenue, Cleveland, OH 44106, USA. E-mail: liming.dai@case.edu*

This journal is © The Royal Society of Chemistry 2014

Energy Environ. Sci., 2014, 7, 1297–1306 | **1297**

poly(styrenesulfonate), PEDOT:PSS), self-assembled monolayers (e.g. 3,3,3-trifluoropropyltrichlorosilane) and metal oxide inorganic semiconductors (e.g. NiO, MoO_3, V_2O_5, WO_3), have been used as HELs.[15–17] The most widely used HEL in PSCs is PEDOT:PSS. However, PEDOT:PSS suffers from its strong acidity (pH = 1–2) and hygroscopicity, etching the indium tin oxide (ITO) electrode to cause degradation of the device efficiency and lifetime.[18,19] On the other hand, the metal oxide inorganic semiconductors often need to be thermally deposited under high vacuum and are incompatible with the high throughout roll-to-roll process of PSCs. Therefore, recent efforts have been devoted to developing solution-processable metal oxide semiconductors by the sol–gel approach or colloid nanoparticle approach.[20–22] The materials used as EELs include low work function metals or related salts (e.g. Ca, LiF), metal oxide semiconductors (e.g. TiO_2, ZnO), fullerene derivatives, and conjugated polyelectrolytes.[15–17] The conjugated polyelectrolyte EELs have recently given a record high PSC device efficiency[10] while metal oxide semiconductor EELs have been widely used with the additional advantages of resistance to oxygen and moisture as well as optical transparency.

Owing to its extraordinary mechanical, electrical, optical, and thermal properties, the two-dimensional (2D) single-atomic-thick sp^2-hybridized carbon sheet of graphene has quickly emerged as an attractive candidate for energy applications.[23–26] However, graphene sheets without functionalization are insoluble and infusible with limited practical applications. Recent efforts have led to solution-processable graphene oxides (GOs) from exfoliation of graphite powders with strong oxidizing reagents (e.g. HNO_3, $KMnO_4$ and/or H_2SO_4).[27,28] The availability of reactive carboxylic acid groups at the edge and epoxy/hydroxyl groups on the basal plane of GO sheets facilitates functionalization of graphene, allowing tunability of optoelectronic properties while retaining the good solubility in water or polar organic solvents.[29,30] Moreover, GO can be produced and processed in solution at large scale with low cost, particularly attractive for massive applications. Indeed, GO and its derivatives have been demonstrated to be useful in many applications with excellent performance, such as batteries, supercapacitors, fuel cells, solar cells, sensors, catalysts and composite materials.[31–33] Of particular interest, GO materials have been used in every part of PSC devices, including as electrodes, charge extraction layers, and in the active layer.[34–37] In this review, we summarize the development of GO materials as charge extraction layers in PSCs by presenting some rational concepts for the design and development of the GO-based hole- or electron-extraction layer for high-performance PSCs, along with the challenges and perspectives in this emerging research field.

2. Graphene oxide derivatives as the hole extraction layer

In 2010, Li et al.[38] reported the first use of GO as an efficient HEL in PSCs because of its suitable work function and good film-forming property. This work triggered the recent extensive research on GO as charge extraction layers in PSCs. Compared with other charge extraction materials, GO possesses many unique advantages, including its two-dimensional structure, easy functionalization, tunable energy levels, solution processability and low cost. With the various strategies developed for improving GO performance in PSCs, several highly efficient and stable PSCs have been reported with GO as the HEL.

To facilitate the hole collection and extraction at the anode, the hole extraction material should have a proper work function to ensure an Ohmic contact with the donor material for efficient hole transport without increasing the device series resistance. As demonstrated by Li et al.,[38] GO had a work function of −4.7 eV to match well with the poly(3-hexylthiophene) (P3HT) donor material for efficient hole extraction (Fig. 1b). Besides, GO could be uniformly deposited onto an ITO anode (Fig. 1b) simply by spincoating its aqueous solution. The PSC device with P3HT:[6,6]-phenyl-C_{61}-butyric acid methyl ester (PCBM) as the active layer and GO as the HEL (see Fig. 1a) exhibited an open-circuit voltage (V_{OC}) of 0.57 V, short-circuit current density (J_{SC}) of 11.40 mA cm^{-2}, fill factor (FF) of 0.54, and power conversion efficiency (PCE) of 3.5 ± 0.3%. This value of PCE is much higher than that (PCE = 1.8%) of the device without HEL and is fairly comparable to that (PCE = 3.6%) of the device based on the state-of-the-art HEL, PEDOT:PSS (Fig. 1d). With the GO layer thickness increased from 2 nm to 10 nm, the FF of the device dramatically decreased from 0.54 to 0.19 with a concomitant decrease in PCE from 3.5% to 0.9% (Fig. 1e) due to the increased series resistance with increasing thickness arising from the insulating nature of GO. The insulating property of GO and its thickness-dependent performance in PSC devices are disadvantages for GO HEL, which will be addressed later in more detail with possible solutions.

Gao et al.[39] reported the utilization of GO as the HEL in inverted PSCs. The device configuration is shown in Fig. 2a. The uniform GO layer (Fig. 2b) was deposited on the P3HT:PCBM active layer by spincoating its solution in anhydrous butyl alcohol. The inverted PSC device with optimal GO layer thickness (2–3 nm) showed a V_{OC} of 0.64 V, J_{SC} of 8.78 mA cm^{-2}, FF of 0.64, and PCE of 3.60%. This performance is also fairly comparable to that of the PEDOT:PSS-based inverted device (Fig. 2c). These authors further discovered that GO could dope P3HT at the surface of the active layer. This was because GO contains carboxylic groups, phenolic and enolic groups with high content of protons.[40] The heavily doped P3HT thin layer at the interface facilitated the formation of an Ohmic contact between the active layer and the top metal electrode, and hence leads to much enhanced device performance.

As mentioned above, one drawback of the GO HEL is its insulating nature, leading to an increased series resistance with a concomitant decrease in FF and PCE of the resulting device. As shown in Fig. 1, those epoxy and hydroxyl groups on the basal plane of GO disrupt the sp^2 conjugation of the graphene lattice to make GO an insulator.[41] As a result, PSCs based on a P3HT:PCBM active layer and GO HEL always exhibit a FF less than 0.65 while the typical value for high performance PEDOT:PSS-based devices is about 0.70. Besides, the device performance is highly sensitive to the thickness of the GO layer

1298 | Energy Environ. Sci., 2014, **7**, 1297–1306

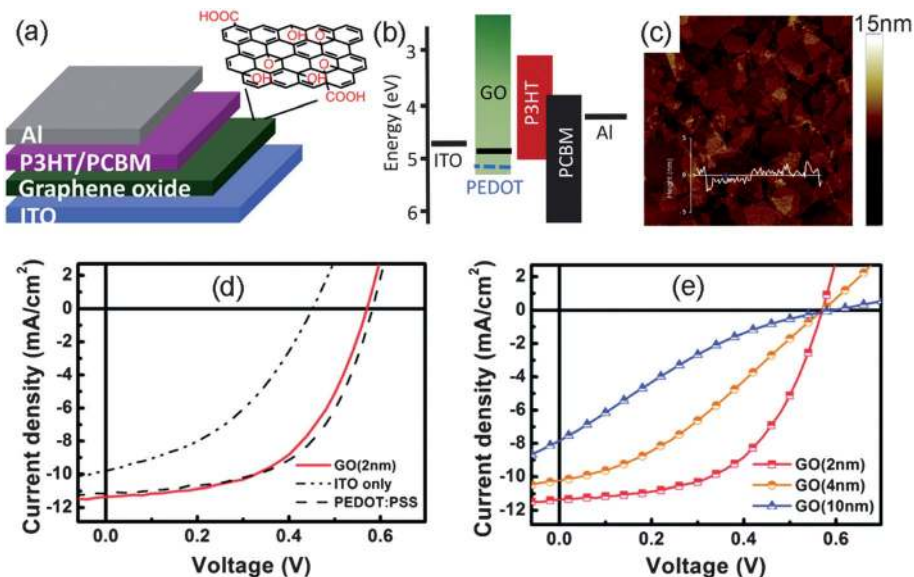This journal is © The Royal Society of Chemistry 2014

Fig. 1   (a) Schematic illustration of the PSC device structure with GO as the HEL. (b) Energy level diagrams of the bottom electrode ITO, interlayer materials (PEDOT:PSS, GO), P3HT (donor), and PCBM (acceptor), and the top electrode Al. (c) An AFM height image of a GO thin film with a thickness of approximately 2 nm. (d) Current density–voltage (J–V) characteristics of the devices with no HEL, with 30 nm PEDOT:PSS film, and with 2 nm GO film. (e) J–V characteristics of the ITO/GO/P3HT:PCBM/Al devices with the GO layer of different thicknesses. Adapted from ref. 38 with permission from the American Chemical Society.
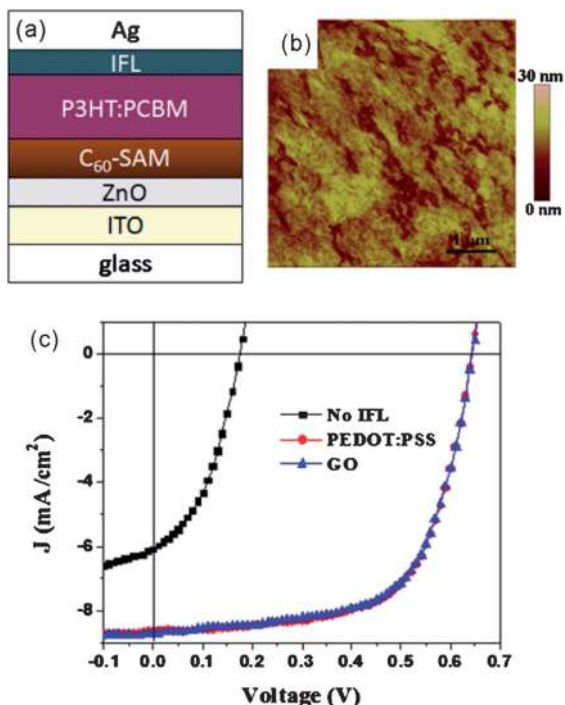

Fig. 2   (a) Device configuration of the inverted PSCs using the GO interfacial layer (IFL) as the HEL. (b) AFM height image of the GO layer on glass/ITO/ZnO/C_{60}-SAM/P3HT:PCBM stacks. (c) J–V characteristics of the inverted PSCs without an interface layer, with a 50 nm PEDOT:PSS layer, and with a 2.1 nm GO layer. Reproduced from ref. 39 with permission from American Institute of Physics.

(see Fig. 1e).[38] To construct high-performance PSC devices with GO as the HEL, therefore, the conductivity of the GO layer must be significantly improved.

The post-oxidation reduction to remove the oxygen-containing groups for recovering the conjugated structure of the basal plane has been utilized to improve the GO conductivity.[42] It has been found that GO could be reduced into r-GO by various approaches, including thermal annealing, microwave irradiation, laser irradiation, and chemical reduction in solution. A large variety of reagents, such as hydrazine, $NaBH_4$, vitamin C, KOH, and HI, have been used to chemically reduce GO in solution.[43] The solution-reduction of GO into reduced graphene oxide (r-GO) is highly compatible with the solution-based fabrication of PSCs. However, r-GO with a reduced number of oxygen-containing groups often exhibits poor solubility in common solvents and tends to form aggregates in the dispersion. Hence, r-GO cannot afford a uniform thin film deposition by spincoating. The poor solubility of r-GO prevents its application as the solution-processed HEL in PSCs. Several approaches, including development of soluble reduced graphene oxide with specific reduction reagents,[44–46] post-treatment of GO film for reduction after spincoating GO aqueous solution,[47,48] and introducing some highly conductive filler to the GO thin film,[49] have been demonstrated to effectively circumvent the poor solubility of r-GO.

Yun et al.[44] developed a solution-processable reduced graphene oxide (pr-GO) through reducing GO with p-toluene-sulfonyl hydrazide in an aqueous solution. pr-GO was demonstrated to be an excellent HEL for efficient and stable PSCs. For comparison, they also prepared normal r-GO by reducing GO with hydrazine as widely used in the literature.[28] Both pr-GO and r-GO showed about 10^5 times higher conductivity than that of GO. Like GO, pr-GO could also be uniformly solution-cast on the ITO surface. In contrast, r-GO could not afford a uniform film deposition and formed large aggregates
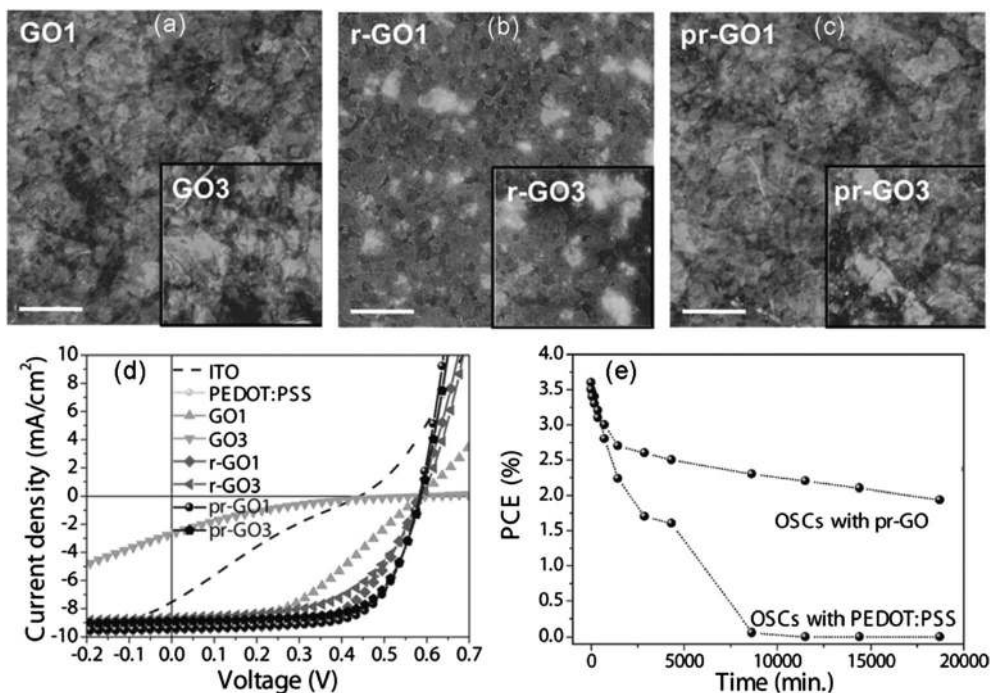
Fig. 3 AFM height images of GO (a), r-GO (b), and pr-GO (c) spincoated on the ITO electrode. (d) $J-V$ characteristics of the PSC devices with GO, r-GO, and pr-GO as the HEL. (e) Changes in PCE of a conventional PEDOT:PSS-based PSC device and a pr-GO-based PSC device during exposure to air. Reproduced from ref. 44 with permission from John Wiley and Sons.
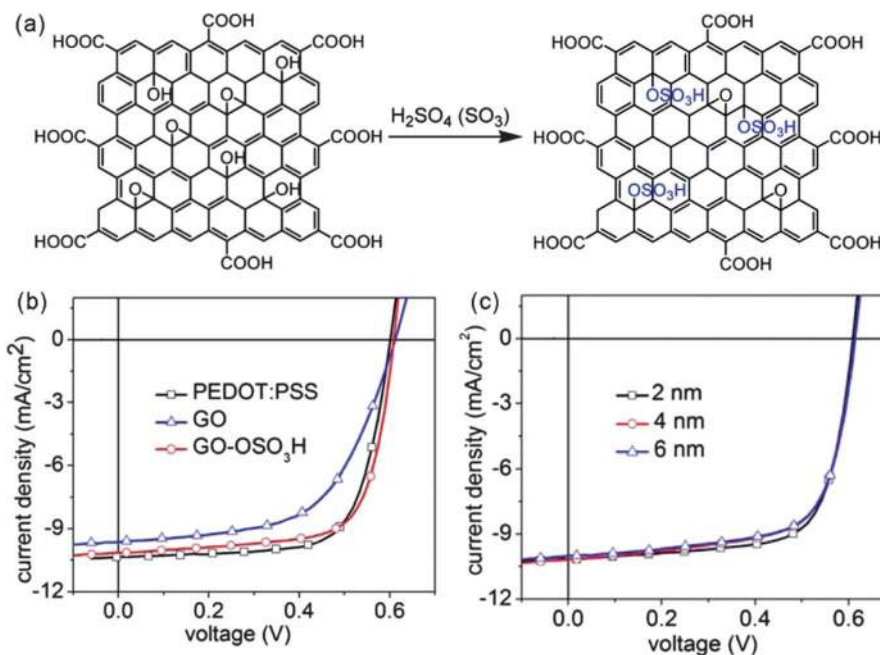

Fig. 4 (a) Schematic structure and synthetic route to GO-OSO$_3$H. (b) $J-V$ curves of the PSC devices with PEDOT:PSS (25 nm), GO (2 nm), or GO-OSO$_3$H (2 nm) as the HEL. (c) $J-V$ curves of the PSC devices with GO-OSO$_3$H as the HEL with different thicknesses. Reproduced from ref. 45 with permission from the American Chemical Society.

on the ITO surface (Fig. 3a–c). Consequently, pr-GO exhibited much better PSC device performance than those of GO and r-GO (Fig. 3d). The PSC device with P3HT:PCBM active layer and pr-GO as the HEL showed a PCE of 3.63% with the FF of 0.667, J_{SC}

of 9.33 mA cm^{-2}, and V_{OC} of 0.59 V, which was highly comparable to its PEDOT:PSS counterpart. Moreover, the pr-GO-based device manifested much longer lifetime than that of the PEDOT:PSS-based device (Fig. 3e).

1300 | *Energy Environ. Sci.*, 2014, **7**, 1297–1306

This journal is © The Royal Society of Chemistry 2014

Liu et al.[45] reported a rationally designed solution processable sulfated graphene oxide (GO-OSO$_3$H) synthesized by treating GO with fuming sulfuric acid to introduce –OSO$_3$H groups onto the reduced basal plane of GO (Fig. 4a). These authors found that the dehydration effect of fuming sulfuric acid resulted in reduction of the carbon basal plane and enhanced conductivity (1.3 S m^{-1} for GO-OSO$_3$H vs. 0.004 S m^{-1} for GO). Furthermore, the newly introduced –OSO$_3$H groups, along with the existing –COOH groups in GO, rendered GO-OSO$_3$H soluble (1 mg mL^{-1} DMF solution) for solution processing. In addition, the protons in –OSO$_3$H groups and –COOH groups in GO-OSO$_3$H gave rise to surface doping of P3HT in the active layer.[40] As a result, PSC devices with GO-OSO$_3$H as the HEL showed excellent device performance with an extraordinarily high FF of 0.71, V_{OC} of 0.61 V, J_{SC} of 10.15 mA cm^{-2}, and PCE as high as 4.37% (Fig. 4b). This performance is among the highest reported for PSC devices with the P3HT:PCBM active layer. Moreover, the device performance was nearly independent of the GO-OSO$_3$H layer thickness (Fig. 4c), which was in stark contrast to the aforementioned device with the insulating GO as the HEL.

Apart from the aforementioned approaches, post-thermal annealing of the preformed GO film has also been demonstrated to obtain reduced GO thin film with enhanced conductivity. During thermal annealing, oxygenated functional groups in GO can be removed via release of gas molecules (e.g. H$_2$O, CO$_2$, CO)

from the reduced carbon basal plane.[43] However, this approach is limited to PSC devices on glass substrates. Plastic substrates in flexible PSCs cannot tolerate the high temperature (200–300 °C) required for the thermal GO reduction.

Joen et al.[47] demonstrated efficient PSCs with thermally annealed GO layer as the HEL. The GO HEL was deposited by spincoating GO aqueous solution on the glass/ITO substrate, followed by thermal annealing at 150 °C, 250 °C or 350 °C for 10 minutes in air. The reduction of GO was confirmed by the dramatic decrease of the C–O peak intensity in the X-ray photoelectron (XPS) spectra (see Fig. 5a and b). Take the thermal annealing at 250 °C as an example, the GO film conductivity increased from 8 × 10^{-6} S m^{-1} to 1.8 S m^{-1} after the reduction by thermal annealing. Consequently, the PCE of the PSC device increased from 1.47% to 3.98%, which was fairly comparable to that of the control device with PEDOT:PSS as the HEL. Moreover, the device based on thermally annealed GO exhibited much better stability than the PEDOT:PSS-based device. Liu et al.[48] had systematically investigated the influence of the preparation conditions of GO HEL on the PSC device performance. They also found that high temperature (230 °C) treatment of GO HEL after spincoating increased the GO layer conductivity and greatly improved the FF and PCE of the resulting PSC devices. To make high quality GO films, these authors optimized the concentration and spincoating speed of the GO solution.

In addition to the thermal treatment, other treatments of preformed GO thin films have also been investigated to improve the performance of devices with GO as the HEL. For instance, Murray et al.[50] reported a highly efficient and stable PSC with GO as the HEL and PTB7:PC$_{71}$BM (Fig. 6a) as the active layer. In this case, the GO layer was deposited onto a clean ITO substrate
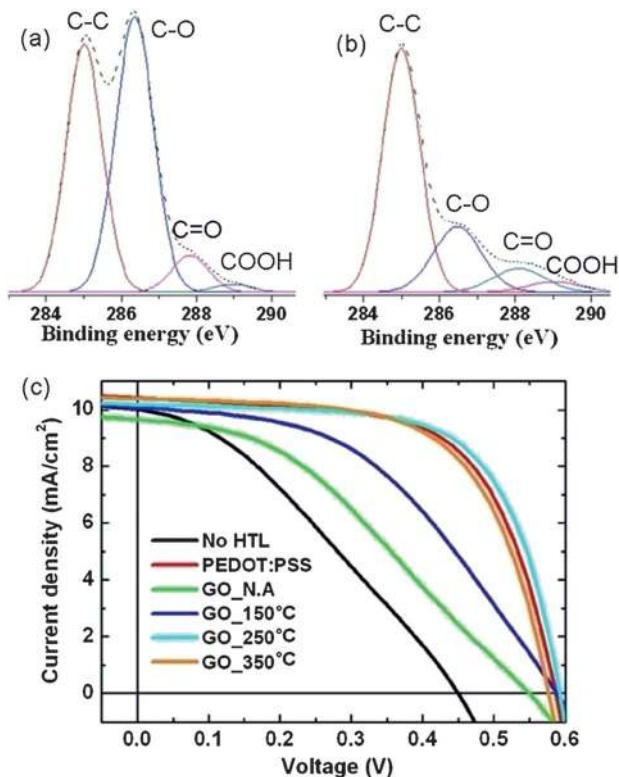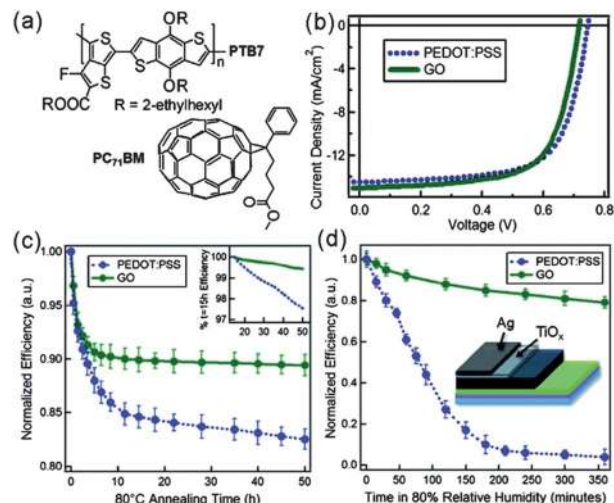

Fig. 5 XPS spectra of GO (a) without thermal treatment and (b) with thermal treatment at 250 °C for 10 minutes. (c) J–V characteristics of PSC devices using thermally reduced GO as the HEL. Reproduced from ref. 47 with permission from Elsevier.

Fig. 6 (a) Chemical structures of the PTB7 donor and PC$_{71}$BM acceptor. (b) J–V plots under AM 1.5 G illumination for PSCs with PEDOT:PSS and GO as the HEL. (c) Thermal degradation of encapsulated devices at 80 °C under an N$_2$ atmosphere. (d) Environmental degradation of unencapsulated devices fabricated with air-stable electrodes at 25 °C under 80% relative humidity. Reproduced from ref. 50 with permission from the American Chemical Society.

with a controlled density *via* Langmuir–Blodgett assembly, followed by low level ozone exposure to modify the GO surface chemistry. These authors found that the GO HEL thus prepared could effectively regulate the PTB7 π-stacking orientation to be favorable for charge extraction. The resultant GO-based device showed a PCE of 7.39%, comparable favorably to the corresponding value of 7.46% for a PEDOT:PSS-based device (Fig. 6b). More importantly, this GO-based device provided a 5 times enhancement in thermal aging lifetime (Fig. 6c) and a 20 times enhancement in humid ambient lifetime (Fig. 6d) with respect to the PEDOT:PSS-based device. Yang *et al.*[51] treated GO HEL with oxygen plasma to change the surface characteristics for an improved PSC efficiency. It was found that the oxygen plasma treatment led to simultaneous enhancements in J_{SC} (9.91 mA cm^{-2} *vs.* 8.42 mA cm^{-2}), V_{OC} (0.60 V *vs.* 0.58 V), and FF (0.60 *vs.* 0.55), and hence a significantly improved PCE (3.59% *vs.* 2.71%), which was attributed to a high work function of the oxygen plasma treated GO for ensuring an increased hole mobility and enhanced hole extraction.

The potential use of conductive fillers to improve the conductivity of GO HELs has also been investigated. In this context, single-walled carbon nanotubes (SWCNTs) with a small diameter of *ca.* 1 nm are particularly attractive because they do not significantly increase the surface roughness of the GO thin film. However, controlling the quality of dispersion to obtain homogenous conductively filled GO films is critical for the

performance of the resultant PSC devices. Kim *et al.*[49] have successfully incorporated SWCNTs into the GO HEL by mixing SWCNTs and GO in water under sonication, followed by spin-coating to yield a uniform GO:SWCNT composite thin film. As can be seen in Fig. 7a, the incorporation of a small amount of SWCNTs increased the through-thickness conductivity of the GO film by an order of magnitude. Therefore, the incorporation of SWCNTs into the GO layer not only improved the device efficiency, but also allowed the use of thicker and easier-to-make GO films. PSC devices with P3HT:PCBM active layer and GO:SWCNT = 1:0.2 as the HEL exhibited a V_{OC} of 0.60 V, J_{SC} of 10.82 ± 0.56 mA cm^{-2}, FF of 0.628 ± 0.0031, and PCE of 4.10 ± 0.18%, which were fairly comparable to those of the PEDOT:PSS-based device (Fig. 7b). Having demonstrated the excellent device performance for GO:SWCNT as the HEL, the same authors further used GO:SWCNT as an interconnect layer for constructing serially connected tandem polymer solar cells with subcells stacked along the optical path to increase optical absorption.[52] The key index of a successful tandem structure is the value of V_{OC}, which ideally should be the sum of V_{OC} of the constituent subcells. Both regular and inverted tandem cells with GO:SWCNT as the interconnect layer were constructed to show a V_{OC} of 84% and 80% of the sum of the two constituent subcells, respectively. These results indicate that successful serial connection of subcells with the GO:SWCNT has been achieved.

In addition to the use of SWCNTs as the conductive filler, PEDOT:PSS has also been blended into the GO HEL for improving the PSC performance.[53–56] As demonstrated by Tung *et al.*,[55] the mixing of GO and PEDOT:PSS in water caused the dispersion to increase its viscosity dramatically, producing a sticky film upon solution casting, due to possible PEDOT chain reorientation around GO sheets. Therefore, tandem PSCs could be fabricated by a direct adhesive lamination process with the sticky conductive GO:PEDOT film. Alternatively, Fan *et al.*[54] have introduced graphene oxide decorated with Au-nanoparticles (Au NPs) into a PEDOT:PSS layer for utilizing the plasmonic effect associated with the Au NPs to increase light absorption and improve the J_{SC} and PCE of the PSC device. The decoration of Au NPs on GO sheets could ensure a uniform dispersion of Au NPs, which otherwise could easily aggregate in a physically blended system.

The use of a GO and metal oxide bilayer HEL has also been demonstrated to show excellent PSC device performance. Indeed, Ryu and Jang[56] reported that PSCs with HELs based on GO, NiO$_x$ and a GO/NiO$_x$ bilayer exhibited PCEs of 2.33%, 3.10%, and 3.48%, respectively. The bilayer structure HEL showed the highest PCE with the V_{OC} of 0.602 V, J_{SC} of 8.71 mA cm^{-2}, and FF of 0.664. Furthermore, Chao *et al.*[57] have successfully used a GO/VO$_x$ bilayer as the HEL to construct high-performance inverted PSCs (Fig. 8a). Inverted PSC devices with solution-processed metal oxide HEL often suffer from a relatively low V_{OC} because of the penetration of metal oxide precursors into the underlying active layer to form defect sites during the film formation by spincoating. To avoid the interfacial penetration, they placed a thin layer of two-dimensional graphene oxide sheet between the active layer and the metal oxide layer. The high LUMO level of the GO interlayer could also block electrons to promote V_{OC} (Fig. 8a). As a result, the P3HT:PCBM-based inverted device with a GO/VO$_x$
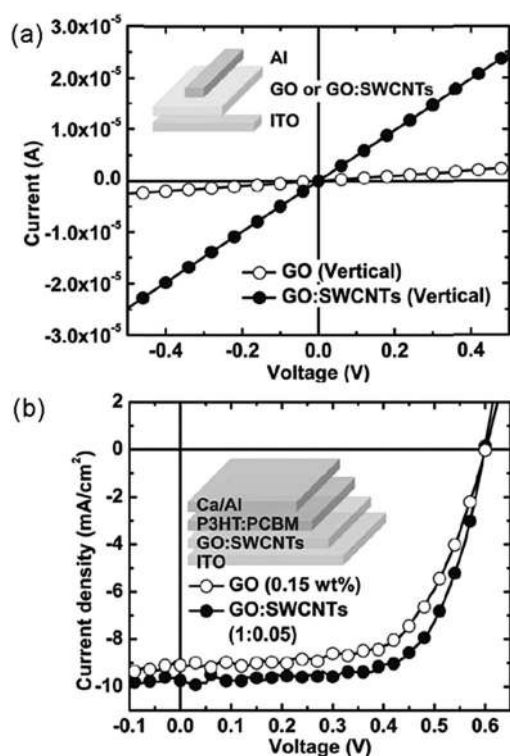

Fig. 7 (a) Addition of a small amount of SWCNTs into the GO film can decrease the through-thickness resistance of the GO film by an order of magnitude. (b) Addition of a small amount of SWCNTs into the GO layer can increase the FF and J_{SC} of devices with GO HEL. Reproduced from ref. 49 with permission from John Wiley and Sons.

1302 | *Energy Environ. Sci.*, 2014, **7**, 1297–1306

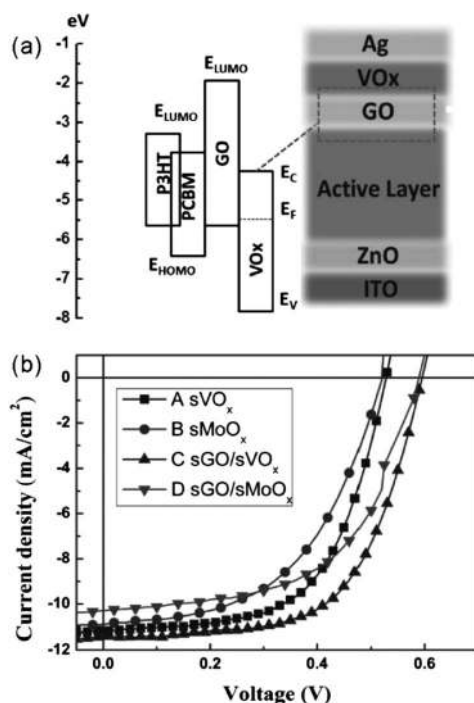This journal is © The Royal Society of Chemistry 2014

Fig. 8 (a) Schematic illustrations of the device architecture and the energy level diagram of solution-processed inverted PSCs with GO/VO$_x$ bilayer as the HEL. (b) J–V characteristics of P3HT:PCBM inverted PSCs with different HELs. Reproduced from ref. 57 with permission from John Wiley and Sons.

(PTh$_4$FBT) as the donor material and bilayer GO/VO$_x$ as the HEL exhibited a PCE of 6.7%, which was fairly comparable to 6.8% of the corresponding control device with vacuum-evaporated MoO$_3$ as the HEL. Besides, Park et al.[58,59] investigated the bilayer structure of GO or r-GO/PEDOT:PSS as the HEL in PSCs, and found that the GO/PEDOT:PSS bilayer showed a better device performance than that of the r-GO/PEDOT:PSS bilayer. This was presumably due to the different work functions of r-GO ($\phi_F = 4.5$ eV) and GO ($\phi_F = 4.7$ eV).

Along with the extensive research on the development of GO derivatives as HELs for high-performance PSCs, Liu et al.[60] have recently developed graphene oxide ribbon (GOR) as the HEL. GOR was prepared by oxidative unzipping of SWCNTs, followed by an extra oxidation process (Fig. 9a). The GOR combined the solution processability of GO and the semiconducting property with a bandgap of graphene ribbon. Cyclic voltammetry of GOR implied a HOMO of -5.0 eV and LUMO of -3.5 eV, which could facilitate hole transporting and electron blocking to minimize the electron–hole recombination on the anode (Fig. 9b). Moreover, GOR showed superior film forming properties on the ITO surface. Consequently, PSCs based on GOR HEL exhibited a V_{OC} of 0.62 V, J_{SC} of 9.96 mA cm^{-2}, FF of 0.67, and PCE of 4.14%. This performance was comparable to that of the PEDOT:PSS-based device and was much better than that of the corresponding GO-based device (Fig. 9c). Furthermore, the PSC devices with GOR as the HEL exhibited a better stability compared to the PEDOT:PSS-based device.

bilayer HEL showed a PCE of 4.1%, outperformed its counterparts with only GO or VO$_x$ as the HEL (Fig. 8b). It was worthy to note that the GO/metal oxide bilayer concept has also been applied to high-efficiency PSCs based on low bandgap polymer donors. An inverted device with a low bandgap polymer

3. Graphene oxide derivatives as the electron extraction layer

While HEL materials should have a high work function, electron extraction layer (EEL) materials should have a low work
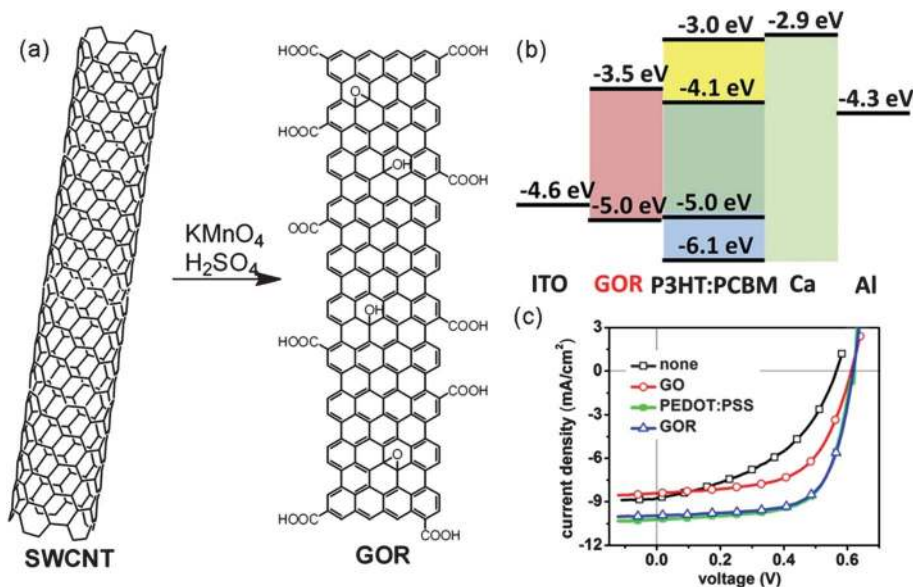

Fig. 9 (a) Schematic illustration of synthesizing graphene oxide ribbon (GOR) by oxidative unzipping of SWCNTs. (b) Energy level alignment of the GOR-based PSC device. (c) J–V curves under AM 1.5 G illumination of the PSCs without and with GO, PEDOT:PSS or GOR as the HEL. Reproduced from ref. 60 with permission from John Wiley and Sons.
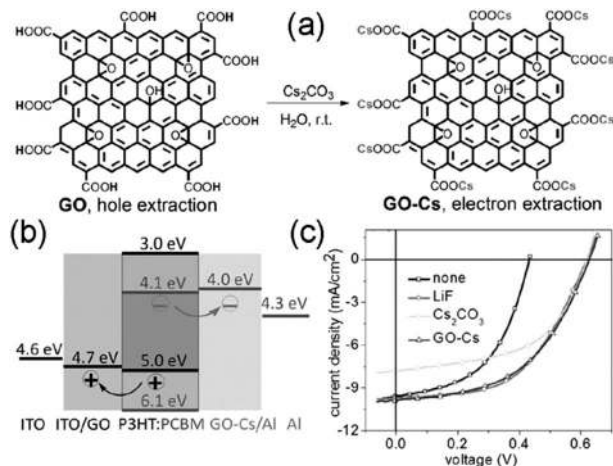
Fig. 10 (a) Schematic structure and synthetic route to GO-Cs. (b) Energy level diagram of the PSC device with GO as the HEL and GO-Cs as the EEL. (c) J–V curves of devices (device structure: ITO/PEDOT:PSS/P3HT:PCBM/EEL/Al) with none, LiF, Cs_2CO_3, and GO-Cs as the EEL. Reproduced from ref. 62 with permission from John Wiley and Sons.

function to match the LUMO level of the acceptor material in the active layer to facilitate electron extraction. Moreover, EELs should efficiently transport electrons to minimize series resistance of the PSC devices for good photovoltaic performance. Being an ambipolar material for efficient transport of both holes and electrons,[61] GO derivatives with tunable energy levels by functionalization can also be used as the EEL for PSCs. Thus, GO and its derivatives are the first class of charge extraction materials which can be used as both HELs and EELs.

Liu et al.[62] reported the first GO-based electron extraction material by using the cesium-neutralized graphene oxide (GO-Cs) as the EEL for PSCs. As schematically shown in Fig. 10a, upon adding Cs_2CO_3 into an aqueous solution of GO, the periphery –COOH groups on the graphene oxide sheets were neutralized and afforded –COOCs groups in the resultant GO-Cs. GO-Cs modified electrode showed the work function of 4.0 eV, matching well with the LUMO level of the PCBM acceptor. Thus, GO-Cs could be used as the EEL in PSCs. In fact, PSC devices with GO-Cs as the EEL and P3HT:PCBM active layer exhibited fairly comparable V_{OC}, J_{SC}, FF and PCE with those of the corresponding control device with the state-of-the-art EEL (e.g. LiF), indicating that GO-Cs was indeed an excellent EEL. These authors further fabricated regular and inverted PSCs with both GO as the HEL and GO-Cs as the EEL. The regular device (device structure: ITO/GO/P3HT:PCBM/GO-Cs/Al) showed the V_{OC} of 0.61 V, J_{SC} of 10.30 mA cm^{-2}, FF of 0.59, and PCE of 3.67%. The inverted device (device structure: ITO/GO-Cs/P3HT:PCBM/GO/Al) showed the V_{OC} of 0.51 V, J_{SC} of 10.69 mA cm^{-2}, FF of 0.54, and PCE of 2.97%. The normal and inverted devices based on GO hole- and GO-Cs electron-extraction layers both showed comparable photovoltaic performance to the corresponding standard BHJ solar cells with the state-of-the-art hole- and electron-extraction layers.

On the other hand, Qu et al.[63] have developed a r-GO/fullerene composite as the EEL for PSCs. These authors first
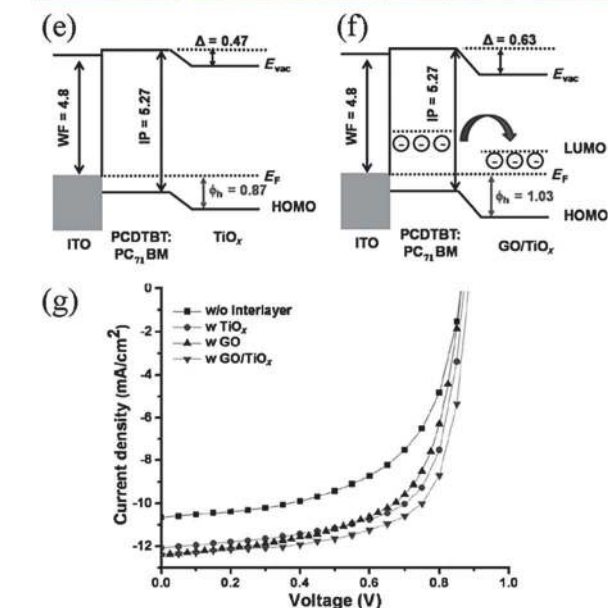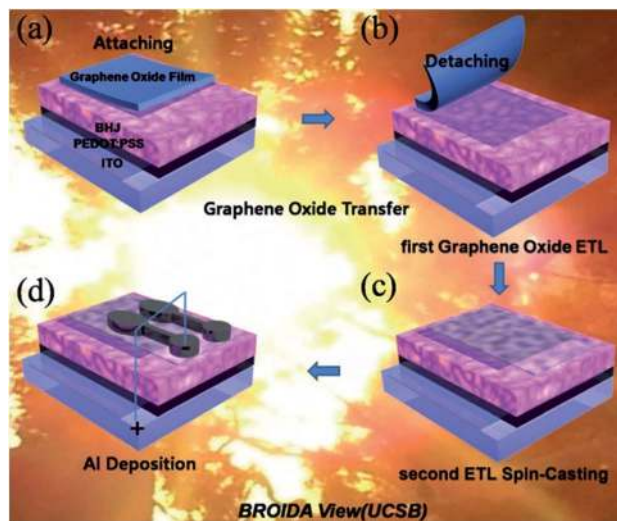

Fig. 11 Schematic illustration of the fabrication steps of BHJ solar cells with GO as the EEL by stamping transfer. (a) Attachment of the transfer film on top of the active layer; (b) after detachment of the film, the first EEL of GO was uniformly transferred and coated onto the active layer; (c) spin-casting TiO_x as the second EEL on top of GO; (d) completed device structure after Al deposition. Energy-level diagrams of the active layer with EELs of TiO_x (e) and GO/TiO_x (f). E_{vac} = vacuum level, E_F = Fermi level, Δ = interfacial dipole, ϕ_h = hole-injection barrier. (g) J–V characteristics of devices without EEL and with the EEL of TiO_x, GO, and GO/TiO_x. Reproduced from ref. 64 with permission from John Wiley.

synthesized a fullerene derivative bearing a pyrene "anchor" unit, which was then non-covalently attached to r-GO via the π–π interaction of the pyrene unit and the r-GO carbon basal plane. PSC devices with the r-GO/fullerene composite as the EEL exhibited a V_{OC} of 0.64 V, J_{SC} of 9.07 mA cm^{-2}, FF of 0.62, and PCE of 3.89%, which was higher than 3.39% of the control device without EEL.

Wang et al.[64] have fabricated highly efficient PSCs with a GO/TiO_x bilayer as the EEL and poly[N-9″-heptadecanyl-2,7-carbazole-alt-5,5-(4′,7′-di-2-thienyl-2′,1′,3′-benzothiadiazole)]

(PCDTBT):[6,6]-phenyl C_{71} butyric acid methyl ester ($PC_{71}BM$) as the active layer. For the device fabrication (Fig. 11a–d), a GO layer was deposited by graphene stamping transfer from copper foil with a thermal-release tape, followed by oxidation with HNO_3. The PSC device thus fabricated showed a PCE as high as 7.5%, along with a V_{OC} of 0.88 V, J_{SC} of 12.40 mA cm^{-2}, and FF of 0.68. The GO layer was reported to have a proper work function of 4.3 eV, close to the LUMO energy level of $PC_{71}BM$, leading to efficient electron transport. Thus, the GO layer played an important role in improving the J_{SC} and PCE. Furthermore, the device with GO exhibited a much higher stability (3% PCE decay) than the corresponding device without the GO interlayer (56% PCE decay).

4. Concluding remarks

Charge extraction layers play an important role in improving the power conversion efficiency and lifetime of PSCs. Owing to their excellent solution processability, unique two-dimensional structure, functionalization-induced work function tunability, and ambipolar transporting ability, GO and its derivatives have quickly emerged as a new class of efficient hole and electron extraction materials in PSCs. We have summarized recent progress in this newly emerging and exciting research field. As HELs, GO materials have showed better performance than the state-of-the-art HEL (i.e. PEDOT:PSS) and are very competitive with other novel HELs, including the solution processable metal oxides. For the EEL application, GO has already showed great promise, though it is still a research field in infancy.

Current research on GO as a charge extraction layer focuses on PSC devices with P3HT:PCBM as the active layer and ITO as the electrode. However, P3HT:PCBM suffers from low device efficiency while many highly efficient donor or acceptor materials have already been developed.[65,66] ITO will not be the ultimate choice for transparent electrodes of flexible PSCs because of its high cost and brittleness. Various transparent electrodes based on conducting polymers, metal nanowires, carbon nanotubes, and graphene have emerged as the flexible electrode to replace ITO.[67,68] Therefore, novel GO-based charge extraction layers should be developed to match the newly developed efficient donor and acceptor materials in the active layer and the new transparent electrodes. For instance, new efficient donor materials always have lower-lying HOMO level than that of P3HT. For GO to form Ohmic contact with these donor materials to facilitate hole extraction, the work function of GO needs to be lowered. In contrast to the hydrophilic ITO electrode, graphene transparent electrodes are often hydrophobic with which the deposition of a thin film of GO as the charge extraction layer by solution processing is difficult, if not impossible. Hence, hydrophobic GO charge extraction layers need to be developed to match graphene electrodes. The combination of GO and its derivatives with other charge extraction materials will likely afford superior PSC device performance. Continued research efforts in this emerging field could give birth to a flourishing area of photovoltaic technologies.

Acknowledgements

Notes and references

1 G. Yu, J. Gao, J. C. Hummelen, F. Wudl and A. J. Heeger, *Science*, 1995, **270**, 1789–1791.

2 B. C. Thompson and J. M. J. Fréchet, *Angew. Chem., Int. Ed.*, 2007, **47**, 58–77.

3 Y. Y. Liang, Z. Xu, J. B. Xia, S. T. Tsai, Y. Wu, G. Li, C. Ray and L. P. Yu, *Adv. Mater.*, 2010, **22**, E135–E138.

4 H. Y. Chen, J. H. Hou, S. Q. Zhang, Y. Y. Liang, G. W. Yang, Y. Yang, L. P. Yu, Y. Wu and G. Li, *Nat. Photonics*, 2009, **3**, 649–653.

5 K. H. Hendriks, G. H. L. Heintges, V. S. Gevaerts, M. M. Wienk and R. A. J. Janssen, *Angew. Chem., Int. Ed.*, 2013, **52**, 8341–8344.

6 B. Azzopardi, C. J. M. Emmott, A. Urbina, F. C. Krebs, J. Mutale and J. Nelson, *Energy Environ. Sci.*, 2011, **4**, 3741–3753.

7 F. C. Krebs, T. D. Nielsen, J. Fyenbo, M. Wadstrøm and M. S. Pedersen, *Energy Environ. Sci.*, 2010, **3**, 512–525.

8 G. Li, R. Zhu and Y. Yang, *Nat. Photonics*, 2012, **6**, 153–161.

9 H. J. Park, H. Kim, J. Y. Lee, T. Lee and L. J. Guo, *Energy Environ. Sci.*, 2013, **6**, 2203–2210.

10 Z. C. He, C. M. Zhong, S. J. Su, M. Xu, H. B. Wu and Y. Cao, *Nat. Photonics*, 2012, **6**, 591–595.

11 J. B. You, L. T. Dou, K. Yoshimura, T. Kato, K. Ohya, T. Moriarty, K. Emery, C. C. Chen, J. Gao, G. Li and Y. Yang, *Nat. Commun.*, 2013, **4**, 1446–1455.

12 L. S. Hung and C. H. Chen, *Mater. Sci. Eng., R*, 2002, **39**, 143–222.

13 H. Park, S. Chang, M. Smith, S. Gradečak and J. Kong, *Sci. Rep.*, 2013, **3**, 1581.

14 R. Steim, F. R. Kogler and C. J. Brabec, *J. Mater. Chem.*, 2010, **20**, 2499–2512.

15 H. L. Yip and A. K. Y. Jen, *Energy Environ. Sci.*, 2012, **5**, 5994–6011.

16 L. M. Chen, Z. Xu, Z. R. Hong and Y. Yang, *J. Mater. Chem.*, 2010, **20**, 2575–2598.

17 R. Po, C. Carbonera, A. Bernardi and N. Camaioni, *Energy Environ. Sci.*, 2011, **4**, 285–310.

18 M. Girtan and M. Rusu, *Sol. Energy Mater. Sol. Cells*, 2010, **94**, 446–450.

19 M. Jorgensenm, K. Norrrman and F. C. Krebs, *Sol. Energy Mater. Sol. Cells*, 2008, **92**, 686–714.

20 S. Chen, J. R. Manders, S. W. Tsang and F. So, *J. Mater. Chem.*, 2012, **22**, 24202–24212.

21 J. B. You, C. C. Chen, L. Dou, S. Murase, H. S. Duan, S. A. Hawks, T. Xu, H. J. Son, L. P. Yu, G. Li and Y. Yang, *Adv. Mater.*, 2012, **24**, 5267–5272.

22 J. J. Jasieniak, J. Seifter, J. Jo, T. Mates and A. J. Heeger, *Adv. Funct. Mater.*, 2012, **22**, 2594–2605.

23 A. K. Geim and K. S. Novoselov, *Nat. Mater.*, 2007, **6**, 183–191.

24 M. J. Allen, V. C. Tung and R. B. Kaner, *Chem. Rev.*, 2010, **110**, 132–145.

25 D. Chen, H. Zhang, Y. Liu and J. H. Li, *Energy Environ. Sci.*, 2013, **6**, 1362–1387.

26 Y. H. Ng, S. Ikeda, M. Matsumura and R. Amal, *Energy Environ. Sci.*, 2012, **5**, 9307–9318.

27 W. S. Hummers and R. E. Offeman, *J. Am. Chem. Soc.*, 1958, **80**, 1339.

28 S. Park and R. S. Ruoff, *Nat. Nanotechnol.*, 2009, **4**, 217–224.

29 G. Eda and M. Chhowalla, *Adv. Mater.*, 2010, **22**, 2392–2415.

30 Y. Zhu, S. Murali, W. Cai, X. Li, J. W. Suk, J. R. Potts and R. S. Ruoff, *Adv. Mater.*, 2010, **22**, 3906–3924.

31 L. M. Dai, D. W. Chang, J. B. Baek and W. Lu, *Small*, 2012, **8**, 1130–1166.

32 J. Liu, Y. H. Xue, M. Zhang and L. M. Dai, *MRS Bull.*, 2012, **37**, 1265–1272.

33 L. M. Dai, *Acc. Chem. Res.*, 2013, **46**, 31–42.

34 X. J. Wan, G. K. Long, L. Huang and Y. S. Chen, *Adv. Mater.*, 2011, **23**, 5342–5348.

35 A. Iwan and A. Chuchmala, *Prog. Polym. Sci.*, 2012, **37**, 1805–1828.

36 Y. Wang, S. W. Tong, X. F. Xu, B. Özyilmaz and K. P. Loh, *Adv. Mater.*, 2011, **23**, 1514–1518.

37 Y. Li, Y. Hu, Y. Zhao, G. Q. Shi, L. E. Deng, Y. B. Hou and L. T. Qu, *Adv. Mater.*, 2011, **23**, 776–780.

38 S. S. Li, K. H. Tu, C. C. Lin, C. W. Chen and M. Chhowalla, *ACS Nano*, 2010, **4**, 3169–3174.

39 Y. Gao, H. L. Yip, S. K. Hau, K. M. Malley, N. C. Cho, H. Z. Chen and A. K. Y. Jen, *Appl. Phys. Lett.*, 2010, **97**, 203306.

40 Y. Gao, H. L. Yip, K. S. Chen, K. O'Malle, M. O. Acton, Y. Sun, G. Ting, H. Z. Chen and A. K. Y. Jen, *Adv. Mater.*, 2011, **23**, 1903–1908.

41 D. R. Dreyer, S. Park, C. W. Bielawski and R. S. Ruoff, *Chem. Soc. Rev.*, 2010, **39**, 228–240.

42 S. Mao, H. H. Pu and J. H. Chen, *RSC Adv.*, 2012, **2**, 2643–2662.

43 S. F. Pei and H.-M. Cheng, *Carbon*, 2012, **50**, 3210–3228.

44 J. M. Yun, J. S. Yeo, J. Kim, H. G. Jeong, D. Y. Kim, Y. J. Noh, S. S. Kim, B. C. Ku and S. I. Na, *Adv. Mater.*, 2011, **23**, 4923–4928.

45 J. Liu, Y. H. Xue and L. M. Dai, *J. Phys. Chem. Lett.*, 2012, **3**, 1928–1933.

46 H. P. Kim, A. R. B. M. Yusoff and J. Jang, *Sol. Energy Mater. Sol. Cells*, 2013, **110**, 87–93.

47 Y. J. Joen, J. M. Yun, D. Y. Kim, S. I. Na and S. S. Kim, *Sol. Energy Mater. Sol. Cells*, 2012, **105**, 96–102.

48 X. D. Liu, H. Kim and L. J. Guo, *Org. Electron.*, 2013, **14**, 591–598.

49 J. Kim, V. C. Tung and J. X. Huang, *Adv. Energy Mater.*, 2011, **1**, 1052–1057.

50 I. P. Murray, S. J. Lou, L. J. Cote, S. Loser, C. J. Kadleck, T. Xu, J. M. Szarko, B. S. Rolczynski, J. E. Johns, J. X. Huang, L. P. Yu, L. X. Chen, T. J. Marks and M. C. Hersam, *J. Phys. Chem. Lett.*, 2011, **2**, 3006–3012.

51 D. Yang, L. Y. Zhou, L. C. Chen, B. Zhao, J. Zhang and C. Li, *Chem. Commun.*, 2012, **48**, 8078–8080.

52 V. C. Tung, J. Kim and J. X. Huang, *Adv. Energy Mater.*, 2012, **2**, 299–303.

53 B. Yin, Q. Liu, L. Y. Yang, X. M. Wu, Z. F. Liu, Y. L. Hua, S. G. Yin and Y. S. Chen, *J. Nanosci. Nanotechnol.*, 2010, **10**, 1934–1938.

54 G. Q. Fan, Q. Q. Zhuo, J. J. Zhu, Z. Q. Xu, P. P. Cheng, Y. Q. Li, X. H. Sun, S. T. Leeb and J. X. Tang, *J. Mater. Chem.*, 2012, **22**, 15614–15619.

55 V. C. Tung, J. Kim, L. J. Cote and J. X. Huang, *J. Am. Chem. Soc.*, 2011, **133**, 9262–9265.

56 M. S. Ryu and J. Jang, *Sol. Energy Mater. Sol. Cells*, 2011, **95**, 2893–2896.

57 Y. H. Chao, J. S. Wu, C. E. Wu, J. F. Jheng, C. L. Wang and C. S. Hsu, *Adv. Energy Mater.*, 2013, **3**, 1279–1285.

58 Y. Park, K. S. Choi and S. Y. Kim, *Phys. Status Solidi A*, 2012, **209**, 1363–1368.

59 K. S. Choi, Y. Park and S. Y. Kim, *J. Nanosci. Nanotechnol.*, 2013, **13**, 3282–3287.

60 J. Liu, G.-H. Kim, Y. H. Xue, J. Y. Kim, J.-B. Baek, M. Durstock and L. M. Dai, *Adv. Mater.*, 2013, DOI: 10.1002/adma.201302987.

61 S. Wang, P. K. Ang, Z. Q. Wang, A. L. L. Tang, J. T. L. Thompson and K. P. Loh, *Nano Lett.*, 2010, **10**, 92–98.

62 J. Liu, Y. H. Xue, Y. X. Gao, D. S. Yu, M. Durstock and L. M. Dai, *Adv. Mater.*, 2012, **24**, 2228–2233.

63 S. X. Qu, M. H. Li, L. X. Xie, X. Huang, J. G. Yang, N. Wang and S. F. Yang, *ACS Nano*, 2013, **7**, 4070–4081.

64 D. H. Wang, J. K. Kim, J. H. Seo, I. Park, B. H. Hong, J. H. Park and A. J. Heeger, *Angew. Chem., Int. Ed.*, 2013, **52**, 2874–2880.

65 J. Liu, H. Choi, J. Y. Kim, C. Bailey, M. Durstock and L. Dai, *Adv. Mater.*, 2012, **24**, 538–542.

66 T. B. Yang, M. Wang, C. H. Duan, X. W. Hu, L. Huang, J. B. Peng, F. Huang and X. Gong, *Energy Environ. Sci.*, 2012, **5**, 8208–8214.

67 S. Bae, H. Kim, Y. Lee, X. F. Xu, J.-S. Park, Y. Zheng, J. Balakrishnan, Y. Lei, H. R. Kim, Y. I. Song, Y. J. Kim, B. Öyilmaz, J. H. Ahn, B. H. Hong and S. Lijima, *Nat. Nanotechnol.*, 2010, **5**, 574–578.

68 D. S. Hecht, L. B. Hu and G. Irvin, *Adv. Mater.*, 2011, **23**, 1482–1513.